Protein Spreading Kinetics at Liquid−Solid Interfaces via an Adsorption Probe Method†

Maria M. Santore* and Christian F. Wertz

Department of Polymer Science and Engineering, University of Massachusetts, 120 Governors Drive, Amherst, Massachusetts 01003

Received April 20, 2005. In Final Form: July 1, 2005

We report the areal growth kinetics of fibrinogen adsorbed on model hydrophobic and hydrophilic surfaces measured via an adsorption probe method. This approach exploits the adsorption of probe molecules to determine the evolution of fibrinogen test molecules under conditions where the fibrinogen test molecules adsorb at relatively dilute surface conditions, minimizing interactions between them. It is found that fibrinogen test molecules spread from an average initial footprint of 100 nm^2 to a final footprint near 500 nm^2 per molecule on the hydrophobic surface, with a single-exponential decay of 1735 s. On a hydrophilic monolayer, the area increases from 100 to 160 nm^2 with a characteristic time of 6740 s. These results demonstrate the power of the adsorption probe approach and comprise the first measurements of the averaged area relaxations of adsorbed proteins. The observation of single-exponential dynamics is remarkable, given the extensive relaxation on the hydrophobic surface, which must involve fibrinogen denaturing.

Introduction

Protein adsorption has long been a focus of research because of its broad biomedical and technological impact: Protein adsorption determines the fate of biomaterials by facilitating cell adhesion or initiating inflammatory response; it facilitates biocatalyst development through enzyme immobilization; it affects pharmaceuticals through separation efficiency; and, through fouling, it affects membrane performance. New applications, still being developed, exploit or are confounded by protein adsorption in microfluidic arrays. As more stringent requirements are placed on interfaces by new technologies, scientists are further prompted for information about protein adsorption that goes beyond the simple question of adsorbed amounts. Key to scientific understanding and new technologies are conformational and dynamic information, including the behavior of proteins in protein mixtures and complex fluids.

When proteins adsorb physically to a surface, they often relax and denature, altering their biological activity and the access of other molecules and cells to the surface.[1−4] The importance of these surface relaxations and reconformations from a dynamic perspective has been recognized through combined experiment and theory: Protein adsorption traces (for instance growing coverage as a function of time, starting with a bare surface and approaching saturation)[5−10] are fit with kinetic models[11−19] containing adsorption, desorption, and surface reconformation steps, to determine the (often first order) rate constants for these processes. The models are elegant in their approach to describing adsorption, for instance using statistical mechanical theory for the local excluded and open area near randomly placed objects. This general approach, which infers spreading or reconformation rate constants from the evolution of the adsorbed amount, imposes a particular kinetic form (for instance first-order kinetics) and particular geometrical features of the proteins themselves.

At the opposite extreme, it would be valuable to observe the relaxation kinetics of adsorbed proteins by direct methods. Spectroscopy and dicroism provide a means to do that, with peaks indicative of protein-surface interactions or structural features of the proteins,[20−25] for instance alpha helix and beta sheet content, and orientation.

† Part of the Bob Rowell Festschrift special issue.

* To whom correspondence should be addressed.

(1) Underwood, P. A.; Steele, J. G.; Dalton, B. A. *J. Cell Sci.* **1993**, *104*, 793−803.
(2) Chinn, J. A.; Posso, S. E.; Horbett, T. A.; Ratner, B. D. *J. Biomed. Mater. Res.* **1991**, *25*, 535−555.
(3) Lindon, J. N.; McManama, G.; Kushner, L.; Merrill, E. W.; Salzman, E. W. *Blood* **1986**, *68*, 355−362.
(4) Schmaier, A. H.; Silver, L.; Adams, A. L.; Fischer, G. C.; Munoz, P. C.; Vroman, L.; Colman, R. W. *Thrombosis Res.* **1984**, *33*, 51−67.
(5) Elgersma, A. V.; Zsom, R. L. J.; Lyklema, J.; Norde, W. *Colloids Surf.* **1992**, *65*, 17−28.
(6) Buijs, J.; vandenBerg, P. A. W.; Lichtenbelt, J. W. T.; Norde, W.; Lyklema, J. *J. Colloid Interface Sci.* **1996**, *178*, 594−605.
(7) Calonder, C.; Tie, Y.; Van Tassel, P. R. *Proc. Natl. Acad. Sci. U.S.A.* **2001**, *98*, 10664−10669.
(8) Shibata, C. T.; Lenhoff, A. M. *J. Colloid Interface Sci.* **1992**, *148*, 485−507.
(9) Lok, B. K.; Cheng, Y. L.; Robertson, C. R. *J. Colloid Interface Sci.* **1983**, *91*, 104−116.
(10) vanEijk, M. C. P.; Stuart, M. A. C. *Langmuir* **1997**, *13*, 5447−5450.
(11) Lundstrom, I.; Elwing, H. *J. Colloid Interface Sci.* **1990**, *136*, 68−84.
(12) Viot, P.; Van Tassel, P. R.; Talbot, J. *Phys. Rev. E* **1998**, *57*, 1661−1667.
(13) Van Tassel, P. R.; Guemouri, L.; Ramsden, J. J.; Tarjus, G.; Viot, P.; Talbot, J. *J. Colloid Interface Sci.* **1998**, *207*, 317−323.
(14) Brusatori, M. A.; Van Tassel, P. R. *J. Colloid Interface Sci.* **1999**, *219*, 333−338.
(15) Szollosi, G. J.; Derenyi, I.; Voros, J. *Phys. A-Stat. Mech. Appl.* **2004**, *343*, 359−375.
(16) Castells, V.; Yang, S. X.; Van Tassel, P. R. *Phys. Rev. E* **2002**, *65*.
(17) Talbot, J. *J. Chem. Phys.* **1997**, *106*, 4696−4706.
(18) Kurrat, R.; Prenosil, J. E.; Ramsden, J. J. *J. Colloid Interface Sci.* **1997**, *185*, 1−8.
(19) Beissinger, R. L.; Leonard, E. F. *J. Colloid Interface Sci.* **1982**, *85*, 521−533.
(20) Norde, W.; Favier, J. P. *Colloids Surf.* **1992**, *64*, 87−93.
(21) Buijs, J.; Norde, W.; Lichtenbelt, J. W. T. *Langmuir* **1996**, *12*, 1605−1613.
(22) Norde, W.; Giacomelli, C. E. *J. Biotechnol.* **2000**, *79*, 259−268.
(23) Vermeer, A. W. P.; Norde, W. *J. Colloid Interface Sci.* **2000**, *225*, 394−397.
(24) Kim, G.; Gurau, M. C.; Lim, S. M.; Cremer, P. S. *J. Phys. Chem. B* **2003**, *107*, 1403−1409.
(25) Kim, G.; Gurau, M.; Kim, J.; Cremer, P. S. *Langmuir* **2002**, *18*, 2807−2811.

10.1021/la051059s CCC: $30.25
Published on Web 08/10/2005

Relevant to the model system in the current paper, on titania an increase in β-sheet at the expense of α-helix is seen for fibrinogen.[26] This type of information, together with measurements of evolving bioactivity,[1−3,27,28] provide an important perspective on interfacial protein denaturing and the influence of a surface on the protein conformation and solution-accessible protein sites. Information on internal protein structure and bioactivity alone, however, describes the consequences of interfacial protein denaturing, without providing predictive insight, for instance on competitive adsorption.

Direct time-resolved measurements of interfacial protein footprints compliment structural studies but also possess predictive power. Knowledge of the effective protein footprint and relaxation (spreading) rate could be used to anticipate protein coverages in single protein adsorption[29,30] and competitive[4,31] protein adsorption scenarios. Directly measured fundamental spreading rate laws may also form the basis for predicting the "history dependence"[7,32] of protein adsorption. Finally, areal growth information may also be correlated with bioactivity in a way that anticipates the effect of adsorption history on bioactivity.

Of the potential methods to measure the molecular area of adsorbed proteins, atomic force microscopy (AFM), is the obvious choice. Many groups have effectively used this tool to provide static images,[33−38] and some achieve, at great care to remove tip-related artifacts, quantitatively precise measures of feature sizes.[39] Most recently, fibrinogen relaxation has been measured in liquid AFM cells based on the decay of adsorbed protein height or thickness,[40] eliminating the issue of tip artifacts. It is expected that the height-based relaxations should occur on the same time scales as the footprint growth,[40] which we prove here to be the case. Precise, in-situ kinetic (minute resolution) footprint measurements, however, are still beyond the capabilities of the best AFMs, since the liquid cells do not typically maintain well-defined deposition rates and short time kinetics require knowledge of when proteins first adsorbed. Also problematic, weakly bound proteins adsorbed at short times can be transferred to the tip[41] or otherwise perturbed,[38,42] and quantitative areal footprint measurements require tedious tip deconvolution.[39,43] Conclusive interpretation of AFM results also requires the user to track the spreading of many different molecules, (a disadvantage because of the time commitment, but an advantage because of the information gained) since populations with different behaviors (for instance those initially adsorbing end-on versus side-on) may display different relaxation kinetics and different end states.

An alternate approach in the current study employs an adsorption-based probe of interfacial protein spreading rates, where the spreading of the test species is decoupled from the adsorption kinetics of those molecules. This protocol is substantially different from studies employing a continuous adsorption history (from bare substrate to saturated interface) and inferring spreading rates, either from a model with predetermined form or semiquantitatively, through data scaling.[29,44] The current approach also accesses the large-spreading limit in which isolated proteins can experience the maximum substrate contact without interference from neighboring proteins, providing biophysical insight into a new regime and potential future correlations with dynamic force spectroscopy of adsorbed proteins.

The current study examines the interfacial relaxation of fibrinogen on model hydrophobic and hydrophilic monolayers employing the adsorption probe approach. Although the mechanics of the adsorption experiment itself are similar to those in the literature,[8,9,29,44] the key in the current studies is the use of two distinct protein populations and an adsorption history that isolates the arrival period of the test molecules to a time interval short in comparison with the relaxation time. Here we demonstrate that the spreading kinetics of fibrinogen test molecules are independent of the choice of probe molecule (fibrinogen itself or lysozyme), report an average spreading rate law, and determine the substrate-dependent ultimate molecular footprints.

Materials and Methods

Bovine plasma fibrinogen, type IV (95% clottable), and chicken egg white lysozyme were purchased from Sigma. Gel electrophoresis on different lots of this fibrinogen revealed no detectible impurities.[45] The current study used the same fibrinogen product from different lots and found consistent results and also consistent results from different lots of the lysozyme. We have previously demonstrated how contaminants (such as fibronectin, up to 5%) would affect our data and its interpretation, and why our protein-handling procedures yield materials of adequate purity.[29] After labeling proteins with fluorescein isothiocyanate (Sigma) at room temperature in a carbonate buffer, free fluorescein and other potential contaminants were removed by size exclusion chromatography with a BioGel P-6 polyacrylamide gel column, as described previously.[29,46] The column eluent was phosphate buffer such that the purified labeled proteins were at pH 7.4 rather than the pH 9 corresponding to the reaction solution. The extent of fluorescein labeling was measured via absorbance at 494 nm and, for different labeling batches, was between 0.2 ad 0.5 labels per protein molecule.

Buffer solutions employed salts from Fisher Scientific. The phosphate buffer was comprised of 0.008 M Na_2HPO_4 and 0.002 M KH_2PO_4. The carbonate buffer was made of 0.004 M Na_2CO_3 and 0.046 M $NaHCO_3$.

The hydrophobic (C16) and hydrophilic (OH) test surfaces were, respectively, hexadecyltrichlorosilane (from Huls) and (*N*-(3-triethoxysilylpropyl)-4-hydroxybutyramide (from Gelest) self-assembled monolayers deposited on microscope slides, per established procedures.[47,48] The former is a classic alkyl self-

(26) Strehle, M. A.; Rosch, P.; Petry, R.; Hauck, A.; Thull, R.; Kiefer, W.; Popp, J. *Phys. Chem. Chem. Phys.* **2004**, *6*, 5232−5236.
(27) Retzinger, G. S.; Cook, B. C.; Deanglis, A. P. *J. Colloid Interface Sci.* **1994**, *168*, 514−521.
(28) Liu, Q. D.; Frojmovic, M. M. *Biochim. Biophys. Acta-Protein Struct. Mol. Enzymol.* **1998**, *1429*, 217−229.
(29) Wertz, C. F.; Santore, M. M. *Langmuir* **1999**, *15*, 8884−8894.
(30) Nygren, H.; Stenberg, M. *J. Biomed. Mater. Res.* **1988**, *22*, 1−11.
(31) Dejardin, P.; Tenhove, P.; Yu, X. J.; Brash, J. L. *Langmuir* **1995**, *11*, 4001−4007.
(32) Wertz, C. F.; Santore, M. M. *Langmuir* **2002**, *18*, 706−715.
(33) Marchin, K. L.; Berrie, C. L. *Langmuir* **2003**, *19*, 9883−9888.
(34) Sit, P. S.; Marchant, R. E. *Surf. Sci.* **2001**, *491*, 421−432.
(35) Cacciafesta, P.; Humphris, A. D. L.; Jandt, K. D.; Miles, M. J. *Langmuir* **2000**, *16*, 8167−8175.
(36) Sit, P. S.; Marchant, R. E. *Thrombosis Haemostasis* **1999**, *82*, 1053−1060.
(37) Toscano, A.; Santore, M. M. *Langmuir*.
(38) Holland, N. B.; Marchant, R. E. *J. Biomed. Mater. Res.* **2000**, *51*, 307−315.
(39) Eppell, S. J.; Zypman, F. R.; Marchant, R. E. *Langmuir* **1993**, *9*, 2281−2288.
(40) Agnihotri, A.; Siedlecki, C. A. *Langmuir* **2004**, *20*, 8846−8852.
(41) Hemmerle, J.; Altmann, S. M.; Maaloum, M.; Horber, J. K. H.; Heinrich, L.; Voegel, J. C.; Schaaf, P. *Proc. Natl. Acad. Sci. U.S.A.* **1999**, *96*, 6705−6710.
(42) Lea, A. S.; Pungor, A.; Hlady, V.; Andrade, J. D.; Herron, J. N.; Voss, E. W. *Langmuir* **1992**, *8*, 68−73.
(43) Shi, H. Q.; Tsai, W. B.; Garrison, M. D.; Ferrari, S.; Ratner, B. D. *Nature* **1999**, *398*, 593−597.
(44) Wertz, C. F.; Santore, M. M. *Langmuir* **2001**, *17*, 3006−3016.
(45) Malmsten, M.; Johansson, J. A.; Burns, N. L.; Yasuda, H. K. *Colloids Surf. B−Biointerfaces* **1996**, *6*, 191−199.
(46) Wertz, C. F.; Santore, M. M. *Langmuir* **2002**, *18*, 1190−1199.
(47) Chaudhury, M. K.; Whitesides, G. M. *Langmuir* **1991**, *7*, 1013−1025.
(48) Laibinus, P. E. Private communication.

assembled monolayer, whereas the latter is hydroxyl-terminated, being used as a model polar surface. The procedure for the C16 surfaces involved first soaking microscope slides in a 70 vol % H_2SO_4/30 vol % H_2O_2 solution. Slides were then thoroughly rinsed with deionized water and blown dry with nitrogen. After exposure in a Harrick plasma chamber for 20 s, the hydrophobic modification was carried out by placing slides in a desiccator under vacuum for 30 min, resting over a hexadecyltrichlorosilane-containing Petri dish, balanced on the dish edges. OH monolayers were formed on microscope slides after first rinsing them in 95% ethanol and drying in nitrogen, followed by soaking for 30 min in a bath of 40 g of NaOH, 150 mL of milli-Q H_2O, and 200 mL of 95% ethanol. OH SAMs were formed by placing the slides in a bath of 1.0 wt % silane in 95% ethanol and allowing them to sit overnight at room temperature and pressure. They were finally rinsed with 95% ethanol and dried in nitrogen. The water contact angles on the two surfaces were 110° for the C16 surface and 55° for the OH surface.

Protein adsorption on the planar test surfaces was conducted in steady shear laminar flow cells,[8,29] where the shear rate (5 s^{-1}) was sufficiently gentle to avoid perturbation of the protein structure, but provided controlled mass transport and deposition kinetics of proteins on the surfaces. The adsorbed amounts were determined in situ using total internal reflectance fluorescence (TIRF), with calibrations that had been described previously.[29] Briefly, in TIRF, total internal reflection of excitation light inside an optically clear protein-adsorbing substrate sets up an evanescent wave of the excitation light in the nearby solution. In our studies, the characteristic length of the evanescent wave was 100 nm, but could be adjusted through the reflection angle and substrate refractive index. With the length of the evanescent wave substantially exceeding the thickness of the adsorbed protein layer, fluorescent labels on both the adsorbed protein and on proteins free in solution contribute to the fluorescent signal. The signal is, however, dominated by the adsorbed protein, and the fluorescent background from the free molecules is easily subtracted. Our particular TIRF instrument, which has been described in detail previously,[49,50] employs an Ar+ ion laser (488 nm) for excitation and a photon-counting detection system. The microscope slide substrates, which comprise one wall of the adsorption flow cell, are optically coupled to a waveguide prism using index-matching oil. TIRF can be used in single component studies to track adsorption kinetics directly, or labeled populations can be monitored in more complex protocols, to prove competitive behavior.

Results

Adsorption-Probe Approach. Figure 1A demonstrates the experimental procedure, which starts with the injection of a modest amount (relative to surface saturation, 5−5.6mg/m^2)[44] of test protein, in this case fibrinogen on a C16 SAM. Here, the deposition of the test fibrinogen protein (100 ppm) is from flowing phosphate-buffered saline (PBS), which continues to flow after a valve turnover shuts off the flow of test protein. After the test protein is adsorbed, it is allowed to relax on the surface in flowing buffer for a specified time, in this case, 4 h. The surface is then exposed to probe molecules (in this example, the probe is also fibrinogen) that adsorb to the remaining bare surface. The average molecular area of the test molecules (F_t) after the specified aging period is calculated from (N_t) the number of test molecules deposited, (N_p) the number of probe molecules that deposit at the transport limited rate, and (F_p) a characteristic size for the probe molecule

$$F_t N_t + F_p N_p = A \qquad (1)$$

Here A is the total surface area covered. If N_t and N_p are given per unit area, (and the footprints F_t and F_p have the same areal units) then $A = 1$.

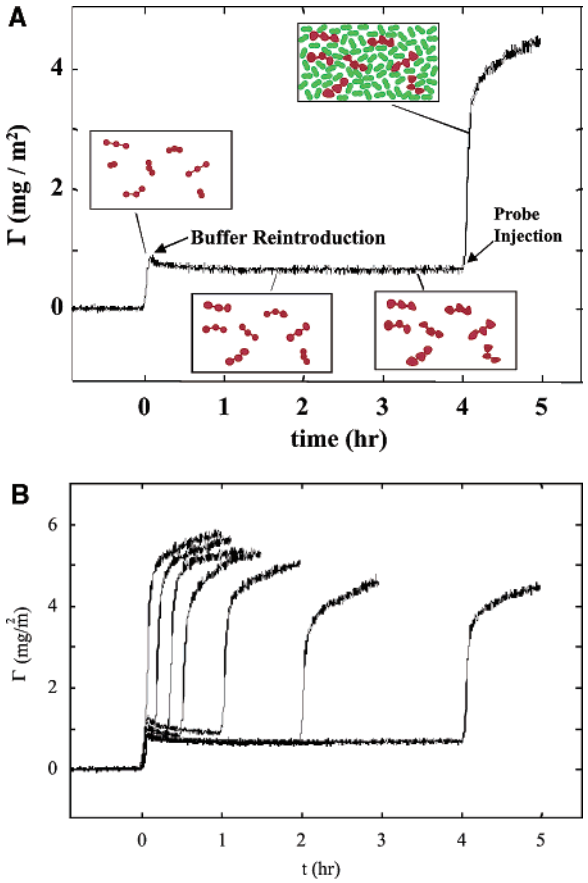

Figure 1. A. Experimental strategy to measure fibrinogen (red) footprint, using probe molecules (green) after controlled relaxation time, in this example, 4 h. Initially buffer flows over the test surface and, at time zero, fibrinogen is injected. Before the surface saturates, buffer solution is reinjected at the first arrow, and the starved fibrinogen layer is allowed to age in pure buffer. At 4 h, the probe molecules are injected. The analysis of surface filling employs the transported limited adsorbed amount of the probe. B. Kinetic traces on a hydrophobic surface, for a range of aging times, employing a fibrinogen probe of fibrinogen spreading.

Repeating the procedure for different aging times of the test molecule allows the determination of the evolving average footprint of the test molecules, F_t. Figure 1B illustrates a full series of runs in which fibrinogen test molecules are probed by subsequent fibrinogen adsorption. Striking in this representation is the convergence of the probe kinetics to a uniform shape for long times of test molecule relaxation, suggesting that, by the end of 4 h, the test molecules are fully relaxed.

The protocol in Figure 1 has several strategic features that facilitate a straightforward analysis: First, the deposition time of the test molecules is short (by almost an order of magnitude) compared with the aging time. This allows one to treat all the test molecules as having arrived to the surface at the same instant (time zero). This instantaneous deposition of test protein is in dramatic contrast to the situation where protein continues to adsorb while the initially adsorbed molecules spread on the surface, leading to continuous populations with different footprints on the surface.[32] (The continuous protein deposition scenario requires deconvolution of protein arrival from spreading kinetics.[10]) In the protocol of Figure 1, different adsorbed populations may form, but completely by chance, as a result of local variations in the substrate

(49) Rebar, V. A.; Santore, M. M. *Macromolecules* **1996**, *29*, 6262−6272.
(50) Kelly, M. S.; Santore, M. M. *Colloids Surf. A-Physicochem. Eng. Aspects* **1995**, *96*, 199−215.

(perhaps resulting from flaws in the slide or in the monolayer chemistry) or as a result of protein orientation at the instant of adhesion. Indeed, it is a general goal of studies such as ours to determine if populations with different spreading kinetics spontaneously evolve.

A second important feature of the experimental design is the relatively rapid probe adsorption. The probe molecule (in this example fibrinogen also) is at a relatively high bulk concentration (100 ppm) so that the interval of probe adsorption is kept short, and that any surface relaxation of the probe minimally contributes to its adsorption kinetics or coverage. Ultimately important is that the probe size and adsorption kinetics be well-defined, as discussed below.

Finally, the current paper attempts to measure the spreading kinetics of test proteins and their ultimate footprints, unhampered by interactions with neighboring test proteins. These fundamental behaviors should depend only on the substrate chemistry, choice of test protein, and the chance of the initial adsorbed conformation. To this end, relatively small amounts of test protein were deposited, less than 20% of the fully saturated surface (for the same surface and bulk conditions). Indeed, for the longest aging times in Figure 1B, substantial adsorption of the probe molecules suggests that large areas of accessible surface remain between the originally adsorbed test molecules, even in their fully relaxed states.

Control experiments were conducted to establish that the initial loading of test protein was sufficiently low such that the kinetics were representative of isolated test molecules. For instance,[51] two runs were compared, in which test protein coverages were 0.8 and 1.8 mg/m^2, corresponding roughly to 20 and 40% of surface saturation. In both runs, the test proteins were allowed to age for 60 min in buffer before being exposed to the injection of probe fibrinogen solution. Quantitative analysis revealed footprints of 374 and 386 nm^2/molecule for the two test runs, with 20 and 40% saturation of the test molecules. This difference of only 3% falls within experimental error. Also worth mentioning, this quantitative consistency between different adsorption histories of fibrinogen argues against multilayer adsorption. Although fibrinogen is known to form networks when activated, the conditions for the current study limited the dominant interactions to those between the protein and the surface.

In the data analysis, the amount of test protein deposited is clear, but the interpretation of the probe size is less obvious: The fibrinogen molecule, 4.5 × 4.5 × 47 nm^3,[3,52] is not an obvious choice of probe and it is not clear what size footprint to assign. This motivated a second probe molecule, lysozyme, 3 × 3 × 4.5 nm^3.[46,53] Indeed, the effectiveness of the adsorption-probe approach relies on the consistent assignment of probe size: the effective probe footprint is more important than its nominal or X-ray crystallographic size.

In this work, we assign probe footprints based on uninterrupted adsorption runs of the probe proteins at bulk concentrations corresponding to the probe portions of runs such as those in Figure 1 onto the same surfaces, in the absence of any test protein. Hence the probe size reflects the dynamics of probe adsorption that occur at the time when the surface begins to jam full of probe (an entirely different quantity from the area excluded by an isolated test protein relaxing on a surface). Figure 2a illustrates the assignment of fibrinogen probe size. At 100 ppm, the same concentration and flow rate used in the probing portions of runs such as Figure 1, fibrinogen adsorption on a bare C16 surface in Figure 2a proceeds at the transport limited rate[9,29,44,54] for 230 s until the fibrinogen coverage reaches 4.1 mg/m^2. Beyond this time, fibrinogen continues to adsorb, but at a slower rate because the molecules already adsorbed to the surface interfere with the approach of additional fibrinogen. Thus, the effective probe footprint for fibrinogen adsorbing at the transport-limited rate is 137 nm^2/ molecule, which falls within the range of expectations from the molecular size, but inherently contains excluded area. Onto an OH SAM, the ultimate fibrinogen coverage and the coverage corresponding to the onset of deviations from transport-limited adsorption (3.5 mg/m^2) are both lower than on the C16 SAM, leading to a larger probe size for fibrinogen on an OH monolayer: 160 nm^2/molecule. This may seem counterintuitive, but the reason is that on the OH monolayer, the kinetic traces deviate from transport-limited behavior sooner (and at lower surface coverages) than on the C16 SAM.

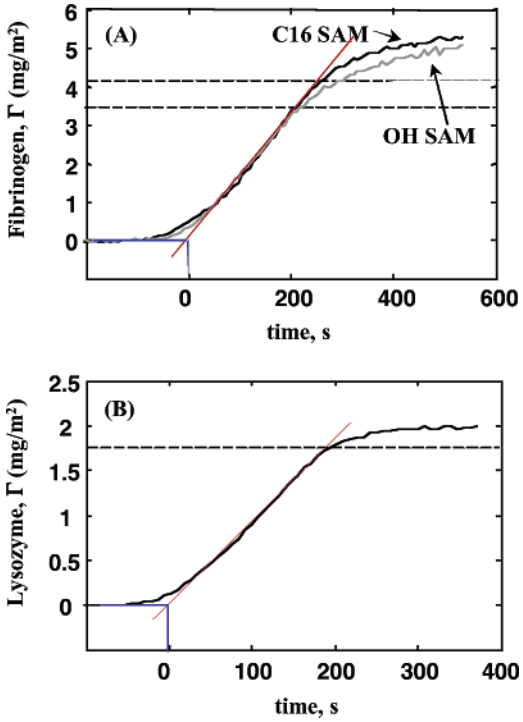

Figure 2. Uninterrupted runs of (A) fibrinogen on C16 and OH SAMs and (B) lysozyme on C16 SAM from 100 ppm fibrinogen solutions. Red line indicates transport-limited rate, and dashed line indicates the coverage where the adsorption rates deviate from the transport-limited rate, identifying an effective footprint for these probe molecules. Time zero is defined by extrapolation of transport-limited kinetics to zero coverage.

In the analysis of data such as that in Figure 1, we employ the molecular footprint for probe fibrinogen of 137 nm^2, but only count the probe molecules (N_p in eq 1) which adhere at the transport-limited rate in the probe portion of Figure 1. Although probe fibrinogen molecules continue to adsorb substantially after the transport-limited regime, these late arriving and slower adhering molecules may be loosely bound or may overlap slightly with molecules already on the surface in ways that are difficult to describe.

It is important to emphasize that the power of the adsorption probe approach lies in the consistency of the

(51) Wertz, C. F., Lehigh University, 2002.
(52) Feng, L.; Andrade, J. D. In *Proteins at Interfaces II*; American Chemical Society: Washington, DC, 1995; Vol. 602, pp 66−79.
(53) Robeson, J. L.; Tilton, R. D. *Langmuir* **1996**, *12*, 6104−6113.
(54) Leveque, A. *Ann. Mines* **1928**, *12*, 201−209.

Table 1. Probes Sizes, Determined from End of Transport-Limited Regime on Bare Surfaces, from Figure 2

probe system	probe size, nm^2
fibrinogen on C16 SAM	137
fibrinogen on OH SAM	160
lysozyme on C16 SAM	12.6

definition of the probe size between the transport-limited parts of calibration runs in which probe molecules adsorb to a bare surface (Figure 2), and the transport-limited parts of runs in which probe molecules adhere to surfaces that are partially blocked by test molecules (Figure 1). Likewise it is important to appreciate that the sizes reported for the test molecules are, in effect, excluded area for the approach of new molecules to the interface. The real question concerns the universality of the area excluded by test molecules. This question motivated the use of a second, extremely different probe molecule, lysozyme. Its probe footprint, based on adsorption to a C16 monolayer was 12.6 nm^2/ molecule, in Figure 2B. Table 1 summarizes probe sizes.

Fibrinogen Spreading Kinetics. Figure 3A presents the areal growth of fibrinogen on the C16 SAM surfaces determined as described above. The footprints on the *y* axis represent the average area per molecule occupied by isolated fibrinogen test proteins and may include molecules possessing different orientations or extents of denaturing. In all cases, the average protein size relaxes from its initial footprint on adsorption to a larger final size. Both lysozyme and fibrinogen probes of fibrinogen relaxation on the hydrophobic surface exhibit qualitatively consistent results, though the fibrinogen probe gives smaller overall values for the apparent size of the fibrinogen test molecules. With two probes of such different chemistries, shapes, sizes, and surface charge (fibrinogen is negative and lysozyme is very positive), the agreement in Figure 3A is strikingly good. Further, we note that the data obtained at this level of analysis agree reasonably with footprint growth determined from an analysis of continuous runs on the same C16 surfaces.[29,44] It is important to note that the test fibrinogen footprint in Figure 3A grows at a relatively rapid rate in its first few minutes on the surface, starting with a footprint near 100 nm^2. On the plateau of Figure 3A, the discrepancy between the lysozyme probe and fibrinogen probe likely stems from relaxations of the fibrinogen probe during the probing process. Since the transport-limited part of the probe injection is about 3−4 min in Figure 1b, for example, the fibrinogen probe itself could grow substantially. This is less of a concern with lysozyme, since the end-on and side-on areas of lysozyme are 9 and 13.5 nm^2, respectively, there is less error associated with the lysozyme measurement.

To reduce error, we did further calculations to account for areal growth of the fibrinogen probe. For fibrinogen adsorbing from a 100 ppm solution, the initial (zero relaxation time) footprint is near 100 nm^2 (from the first pass analysis in Figure 3a, and previously published results[29,44]), and the apparent probe footprint on a bare C16 SAM at the end of the transport-limited regime (230 s, with a coverage of 4.1 mg/m^2) is 137 nm^2. Thus, in the first ~4 min on the surface, the probe size increases by about 37%, and to a first approximation, this increase is linear in time. For the various runs in Figure 1b, however, when the probe is injected, it adsorbs at a transport-limited rate for a period of less than 4 min, because of the previously adsorbed test fibrinogen reduces the open surface area. Hence the effective probe size should be less

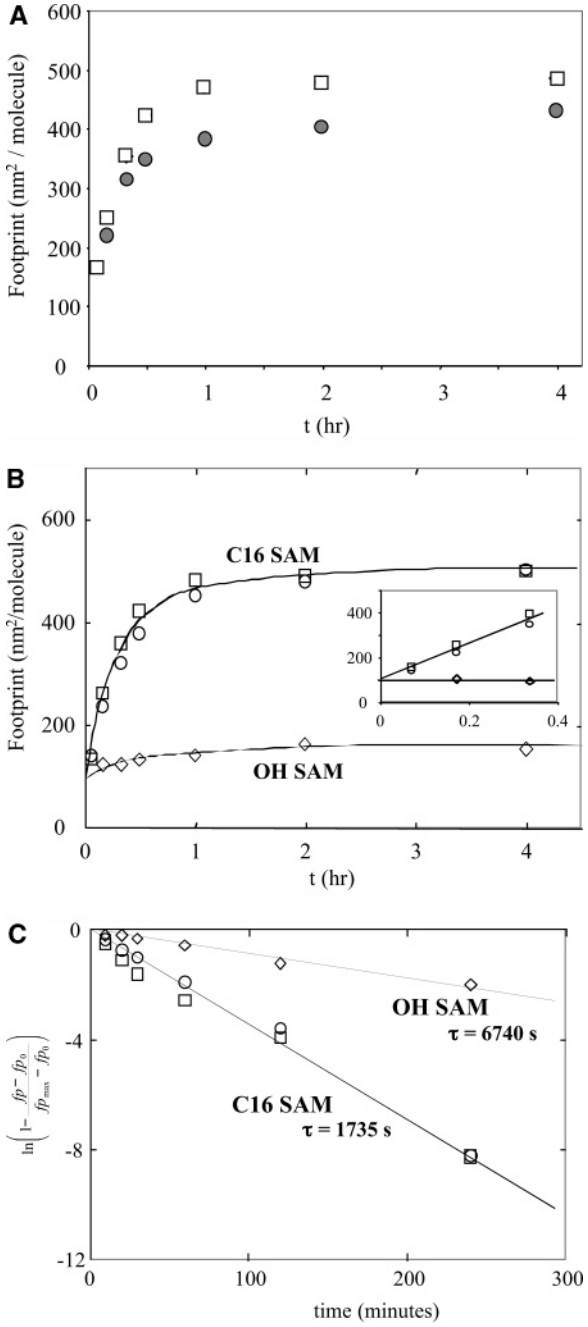

Figure 3. A. Fibrinogen spreading on C16 surfaces, measured by lysozyme probe (squares) and by fibrinogen probe (circles). Here the constant probe sizes are those in Table 1. B. Fibrinogen spreading on C16 and OH SAM surfaces. On the C16 SAM, data are compared for two probes: lysozyme (squares) and fibrinogen (circles), where the size of the latter depends on the duration of the probe injection per Table 2. On the OH SAM, the fibrinogen probe size is that from Table 1, and was found not to vary significantly with the duration of the probe injection. The inset shows how the initial kinetics give an initial footprint near 100 nm^2, independent of surface chemistry. C. Semilog representation of data from panel B demonstrates single exponential relaxation kinetics. Data symbols follow panel B.

than 137 nm^2. In Table 2, we therefore correct the fibrinogen probe size for the runs in Figure 1b to account for the finite adsorption period of the probe molecules, using a linear interpolation between 100 nm^2 for the probe at zero relaxation time, and 137 nm^2 for the (average) probe size at the end of 230s of adsorption. In Table 2, the greatest corrections occur for the longest test protein relaxation. Figure 3b replots the results of fibrinogen probe

Table 2. Corrected Fibrinogen Probe Sizes on C16 SAMs.

relaxation time of test fibrinogen (only identifies the run)	duration of probe injection at T−L rate (s) from Figure 1b	fibrinogen probe size (linearly interpolated) nm^2
10 min	220	135
20 min	210	134
30 min	200	132
60 min	170	127
120 min	130	121
240 min	130	121

on the C16 SAM with the corrected probe size, with the results in striking quantitative agreement with measurements using a 12.6 nm^2 lysozyme probe.

The excellent agreement between the lysozyme and fibrinogen probes of fibrinogen spreading on a C16 SAM argues in favor of the rigor of the probe method and against multilayer adsorption or the influence of protein−protein interactions on the relaxation itself. Although the footprint size on the *y* axis is, technically, an excluded area applying to the approach of new molecules from solution, it has some degree of universality because it applies to equally approaching lysozyme and fibrinogen, despite the obvious differences between the two probe molecules. Data for fibrinogen spreading on the OH monolayer are also included, but because of the relatively small degree of spreading on this more hydrophilic surface, time-based corrections to the fibrinogen probe size had negligible impact.

The results in Figure 3 comprise the first in situ measurements of the average footprint evolution of a protein, after its adsorption onto surfaces of different chemistries. Quantitative protein spreading kinetics with this resolution and time have yet to be achieved with other experimental methods. Furthermore, the data in Figure 3 are powerful because they show the average protein footprint growth, without a priori assumption of a particular mathematical form or relaxation mechanism.

The area relaxation curves for the two surfaces share a common *y* intercept near 100 nm^2, which falls between end-on (4.5 × 4.5 nm = 20.25 nm^2) and side-on (4.5 nm × 47.5 nm = 212 nm^2) fibrinogen configurations. The intermediate initial footprint suggests a combination of initially adsorbed end-on and side-on orientations, as a result of random, nearly surface chemistry-independent encounters of fibrinogen with either surface. Although end-on conformations have not been observed by in situ AFM, their visualization is expected to be difficult: The rapid relaxation away from the initial footprint in Figure 3 on hydrophobic surfaces suggests that the end-on conformation is inherently unstable and would become even more unstable in interactions with an AFM tip on a dilute surface.

Figure 3 demonstrates that, although surface chemistry does not substantially bias the initial adhesion event, it profoundly influences fibrinogen relaxation dynamics and its ultimate footprint. Following initial adsorption on the hydrophobic surface, the molecular fibrinogen area relaxes, via an exponential decay in Figure 3C, to an ultimate footprint near 500 nm^2. This value represents an average of the adsorbed fibrinogen molecules and, strikingly, is five times the original footprint. On the hydrophilic surface, the fibrinogen area grows only to 160 nm^2/molecule, albeit by an exponential decay. Our quantitative observations in Figure 3 are consistent with stationary AFM measurements of fibrinogen on other hydrophobic and hydrophilic surfaces[25] and the observation that displacement of fibrinogen by surfactants is more difficult on hydrophobic surfaces.[5] Figure 3 is also in good quantitative agreement with our previous measurements of protein footprint growth in continuous runs that start with bare surfaces and end with surface jamming. These prior data were limited to the first $^1/_2$ h of the protein relaxation dynamic.[29,44] The current approach goes beyond this to access fully relaxed molecules. Indeed, the fully relaxed sizes of 500 and 160 nm^2 for fibrinogen on the hydrophobic and hydrophilic surfaces are entirely new data as are the exponential decay times.

The differences in the ultimate footprints reflect differences in the specific chemical interactions of fibrinogen with hydrophobic and hydrophilic surfaces. In the case of the hydrophobic surface, the large change in the molecular area suggests reconfigurations beyond a simple falling-over of the adsorbed molecules from an end-on to a side-on conformation of 211 nm^2. Rather, interfacial denaturing occurs, though we have no direct evidence for the extent to which protein domains reorient relative to each other or the extent to which the internal structure of the fibrinogen domains is compromised. Also, as a referee points out, although we know that interfacial denaturing occurs, rollover may also occur (for those proteins initially adsorbed end-on). Indeed, the single-exponential relaxation is remarkable because we do not distinguish different time constants for denaturing and rollover or denaturing of proteins starting end-on versus those starting side-on. This may suggest that denaturing, the process which take the protein all the way to the final state of 500 nm^2, is kinetically dominant. Clearly, hydrophobic attractions between fibrinogen and the surface are large enough to compromise some features of the native protein structure, and indeed it is the loss of fibrinogen's internal physical bonds which must control the relaxation kinetics, through the energy barriers they provide against the relaxation process. In the case of the hydrophilic surface, the area growth is less extensive. Though the current experiments provide no evidence for or against protein denaturing on the hydrophilic surface, it is worth pointing out that the ultimate footprint of 175 nm^2 does not require compromise of fibrinogen structure, since 175 nm^2 lies between the native side-on and end-on adsorbed footprint sizes. Hence, the relaxations on the hydrophilic surface may result simply from interfacial fibrinogen reorientations.

Our findings motivate a comparison to very recent direct measurements of fibrinogen relaxation, measured by height changes in situ with AFM. Agnihotri and Siedlecki[40] recorded height data for different fibrinogen domains as a function of time on mica and hydrophobic graphite, reporting evolution consistent with our observations here: On mica, different side-on conformations were observed, based on the relative heights of the D and E domains, and there was a modest increase in protein height with observation time. This slight reconformation on mica is consistent with our small areal footprint growth on the OH monolayer. By contrast, on the hydrophobic graphite, the molecular heights decreased substantially over their 2-hour observation period, and in the final state, no distinct populations were observed that correlated with the initially adsorbed conformation. These authors fit the relaxation data (taken for up to 28 proteins) to a single-exponential decay model and report a time constant (2127s) for the hydrophobic surface somewhat larger than our own but still within "agreement range", given the uncertainty in the timing of protein-surface contact in the first 10 min in the AFM flowcell, and chemical differences between our C16 surface and graphite.

An additional point is worth noting: Agnihotri and Siedlecki fit their data to a single exponential form rather

than examining the linearity on a semilog plot (as we do in Figure 3C), and therefore, it is not clear from their height relaxation if there are hints of additional relaxation modes besides the main one that we and these authors both observe. Our observation of a *only* a single exponential decay is striking and the AFM data (which obviously measure individual molecules) of Agnihotri and Siedlecki agree with our finding of just one main relaxing mode or population, though our method averages over many molecules.

The single exponential relaxation and large footprint change suggestive of interfacial denaturing on the hydrophobic surface motivate closer examination of fibrinogen relaxation on hydrophobic surfaces. First, given that the compromise of fibrinogen structure likely involves a complex energy landscape involving multiple energy barriers as various internal associations disbond, the single-exponential relaxation comes as a surprise: It is a signature of a single kinetic event with one energy barrier. The rate constant, k, follows from the height of such an energy barrier, or activation energy, E_a, according to the Ahrennius form

$$k = A(T)e^{E_a/k_bT} \quad (2)$$

where $A(T)$ is a preexponential factor with a weak temperature dependence, k_b is Boltzman's constant, and T is temperature in absolute units. The gas-phase preexponential term of k_bT/h (where h is Planck's constant) is not generally valid for solution-phase reactions[26] and would be equally inappropriate for reactions occurring at a solid−liquid interface. For the unfolding of protein molecules, the system is more likely to be in the diffusive regime, consistent with preexponential factors employed in ligand−receptor binding studies: 10^6-10^{12} s^{-1}.[27,28] Choosing an intermediate range of 10^7-10^9 for $A(T)$ therefore yields activation energies between 23 and 28 kT for fibrinogen relaxation on the hydrophobic surface. Such activation energies are consistent with previous reports of other proteins denaturing in solution,[29−31] though large variations in the reported activation energies reflect that the energy needed to compromise internal associations depends substantially on the nature of the particular protein domains being considered.

The two-state (folded and denatured), single energy-barrier model of protein unfolding is common in the literature as a means of analysis and determination of energy barriers, as we report above, and yet it is fundamentally at-odds with the concept of a complex energy landscape an a series of unfolding steps (with a distribution of energy barriers). Although the AFM data of Agnihotri and Siedlecki agree with our macroscopically averaged findings, their data also argue solidly against a two-state model since a time-dependent range of protein heights were reported on graphite. Indeed, the loading-dependent desorption dynamics of our prior studies,[32] also a macroscopically averaged experimental technique, argue against two distinct surface states. Future biophysical studies and theory, therefore, must strive toward an understanding of why the single exponential form for a distribution (rather than a barrier between two states) is prevalent, rather than other forms such as stretched exponential. In the meantime, data such as ours provide solid rationale for the development of models of competitive protein adsorption and biological activity that employ the single-exponential relaxation form.

Summary

This paper described an adsorption-based method, using test and probe populations of adsorbing protein, to determine the areal footprint growth and relaxation kinetics of test proteins. The key to successful area measurements is to employ probe proteins whose adsorption kinetics are well characterized and the transport-limited regime of adsorption is distinct. The probe method does not examine the tight-packed surface conformations of adsorbed proteins, but rather provides a measure of time-dependent excluded surface area. "Occupied" surface area (including the excluded area) is that which prevents adsorption of other proteins at the transport-limited rate. This same criteria is chosen to define the footprints of the probe molecules. Quantitatively consistent results from control studies with different initial loadings of test protein and two dramatically different probe proteins confirm the premise of the method, arguing against multilayer adsorption or specific interactions between proteins on the surfaces.

The current findings with the model fibrinogen test protein on two surfaces of dramatically different hydrophobicity report single exponential relaxation kinetics and strongly surface dependent ultimate footprints. On the hydrophobic surface, where surface−protein interactions are sufficiently strong to compromise the internal protein structure, the average apparent footprint of an isolated fibrinogen molecules can be as large as 500 nm^2. By contrast, on a hydrophilic surface, the ultimate footprint is closer to 160 nm^2.

Acknowledgment. This work was supported by NSF CTS-0242647 and CTS-0428455.

LA051059S